Three-Dimensional Image Fusion of ^{18}F-Fluorodeoxyglucose–Positron Emission Tomography/Computed Tomography and Contrast-Enhanced Computed Tomography for Computer-Assisted Planning of Maxillectomy of Recurrent Maxillary Squamous Cell Carcinoma and Defect Reconstruction

Yao Yu, MD, * *Wen-Bo Zhang, MD,* † *Xiao-Jing Liu, MD,* ‡ *Chuan-Bin Guo, MD, PhD,* § *Guang-Yan Yu, MD, DDS,* ‖ *and Xin Peng, MD, DDS* ¶

Purpose: The purpose of this study was to describe new technology assisted by 3-dimensional (3D) image fusion of ^{18}F-fluorodeoxyglucose (FDG)–positron emission tomography (PET)/computed tomography (CT) and contrast-enhanced CT (CECT) for computer planning of a maxillectomy of recurrent maxillary squamous cell carcinoma and defect reconstruction.

Materials and Methods: Treatment of recurrent maxillary squamous cell carcinoma usually includes tumor resection and free flap reconstruction. FDG-PET/CT provided images of regions of abnormal glucose uptake and thus showed metabolic tumor volume to guide tumor resection. CECT data were used to create 3D reconstructed images of vessels to show the vascular diameters and locations, so that the most suitable vein and artery could be selected during anastomosis of the free flap. The data from preoperative maxillofacial CECT scans and FDG-PET/CT imaging were imported into the navigation system (iPlan 3.0; Brainlab, Feldkirchen, Germany). Three-dimensional image fusion between FDG-PET/CT and CECT was accomplished using Brainlab software according to the position of the 2 skulls simulated in the CECT image and PET/CT image, respectively. After verification of the image fusion accuracy, the 3D reconstruction images of the metabolic tumor, vessels, and other critical structures could be visualized within the same coordinate system. These sagittal, coronal, axial, and 3D reconstruction images were

Received from the Department of Oral and Maxillofacial Surgery, Peking University School and Hospital of Stomatology, Beijing, China.

*Resident.

†Resident.

‡Associate Professor.

§Professor.

‖Professor.

¶Professor.

This work was supported by grants from the National Supporting Program for Science and Technology (No. 2014BAI04B06) and Beijing Municipal Science and Technology Commission (No. Z161100000116053).

Conflict of Interest Disclosures: None of the authors have any relevant financial relationship(s) with a commercial interest.

Address correspondence and reprint requests to Dr Peng: Department of Oral and Maxillofacial Surgery, Peking University School and Hospital of Stomatology, 22 Zhongguancun South Avenue, Beijing 100081, China; e-mail: pxpengxin@263.net

Received January 12 2017

Accepted February 17 2017

0278-2391/17/30222-7

http://dx.doi.org/10.1016/j.joms.2017.02.013

used to determine the virtual osteotomy sites and reconstruction plan, which was provided to the surgeon and used for surgical navigation.

Results: The average shift of the 3D image fusion between FDG-PET/CT and CECT was less than 1 mm. This technique, by clearly showing the metabolic tumor volume and the most suitable vessels for anastomosis, facilitated resection and reconstruction of recurrent maxillary squamous cell carcinoma.

Conclusions: We used 3D image fusion of FDG-PET/CT and CECT to successfully accomplish resection and reconstruction of recurrent maxillary squamous cell carcinoma. This method has the potential to improve the clinical outcomes of these challenging procedures.

J Oral Maxillofac Surg 75:1301.e1-1301.e15, 2017

Resection of recurrent maxillary squamous cell carcinoma (SCC) and defect reconstruction are considered challenging procedures in the field of head and neck reconstructive surgery. Treatment for head and neck cancer often calls for a combined-modality approach that includes surgery, radiation therapy, and chemotherapy. Local persistent or recurrent disease occurs in 30 to 50% of patients with advanced head and neck cancer,[1,2] but the location of the recurrent tumor can be hard to recognize because of scarring due to the prior surgical procedure and radiotherapy. Conventional imaging examinations such as computed tomography (CT) and magnetic resonance imaging are not sensitive for detecting recurrent tumor. Recently, ^{18}F-fluorodeoxyglucose (FDG)–positron emission tomography (PET) has been shown to be useful for staging of SCC of the head and neck.[3] It has high sensitivity and specificity for the detection of nodal metastases[4-6]; moreover, it can differentiate between residual or recurrent disease and normal treatment-induced tissue changes.[7] However, a major disadvantage is that it cannot identify the exact anatomic location of the lesion.[8] The combination of PET and CT has shown promise in this respect, but unfortunately, it cannot provide necessary information on the relationship between the lesion and nearby critical structures.

Radical surgery and radiation therapy cause substantial changes in tissue, distorting normal anatomy and making interpretation of postoperative imaging challenging. Improved methods are needed for detecting local recurrence and accurately locating critical structures in patients with recurrent SCC as the feasibility and success of surgical salvage depend on knowledge of disease extent and involvement of critical structures.

The primary treatment for head and neck cancer often includes radical neck dissection and radiotherapy. During radical neck dissection, several vessels that are commonly used for anastomosis are resected from the root. Because of the radiotherapy, the quality of the vessels in the specific targeting can be influenced. Contrast-enhanced CT (CECT) is one method that can help identify the critical structures near the recurrent tumor, and importantly, it can evaluate the position, length, and diameter of vessels targeted for anastomoses during reconstruction.

The purpose of this article was to describe a new technique of 3-dimensional (3D) image fusion of FDG-PET/CT and CECT for computer-assisted planning of resection of recurrent maxillary SCC and defect reconstruction.

Materials and Methods

A 46-year-old woman who had been diagnosed with SCC of the right maxilla 2 months earlier presented to our institution with a visible right-sided midfacial deformity and limited mouth opening. She had undergone resection of a right lingual SCC 15 years ago, when she received dissection of the right side of the neck without reconstruction, followed by radiation therapy (70 Gy). Distortion of anatomy due to soft tissue scarring and the limited opening mouth made it difficult to define the location and extent of the tumor by clinical examination or CECT scans (Fig 1). An FDG-PET/CT scan showed well-defined tracer accumulation in the right skull-base region, close to the sphenoid sinus (Fig 2). The hypermetabolic region could be exactly localized on the co-registered CT images by matching the landmarks, but the critical structures around the tumor and the recipient vessel for anastomosis of the free flap could not be shown on the CT scan. Three-dimensional image fusion of FDG-PET/CT and CECT was then successfully used to identify the tumor and the vessels in the same reference frame; on the basis of this information, maxillary tumor resection and reconstruction with free anterolateral thigh flap were accomplished.

IMAGE ACQUISITION

The patient was taken to the PET/CT suite on a plate, with the applicators in place. PET/CT was performed on a Discovery STE scanner (GE Healthcare, Milwaukee, WI). Non–contrast-enhanced CT images were first acquired using a 16-slice helical CT scanner

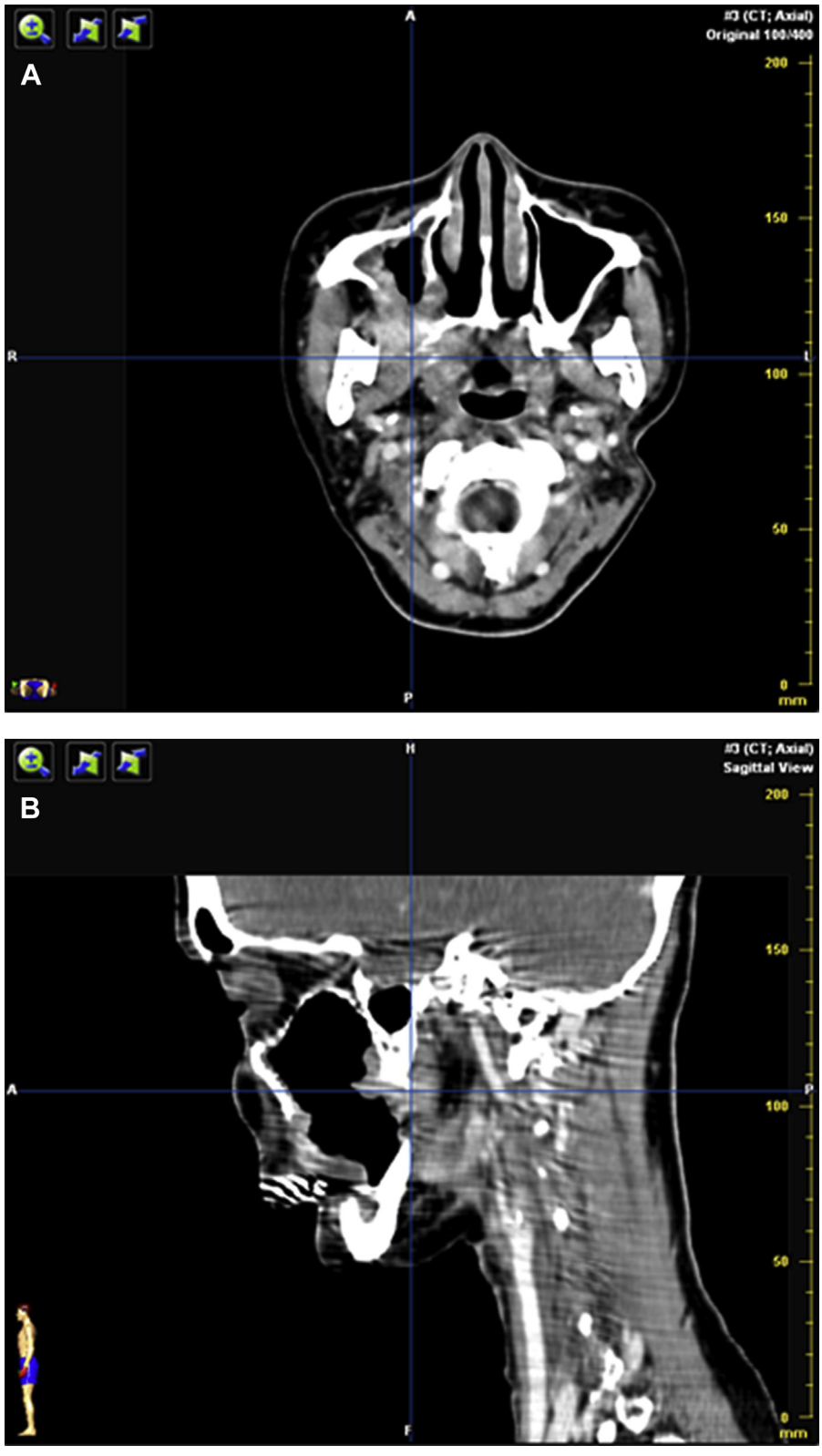

FIGURE 1. Contrast-enhanced computed tomography (CECT) scan images showing the recurrent maxillary squamous cell carcinoma. *A*, Axial view of CECT. *B*, Sagittal view of CECT. **(Fig 1 continued on next page.)**

Yu et al. Computer-Assisted Planning of Maxillectomy. J Oral Maxillofac Surg 2017.

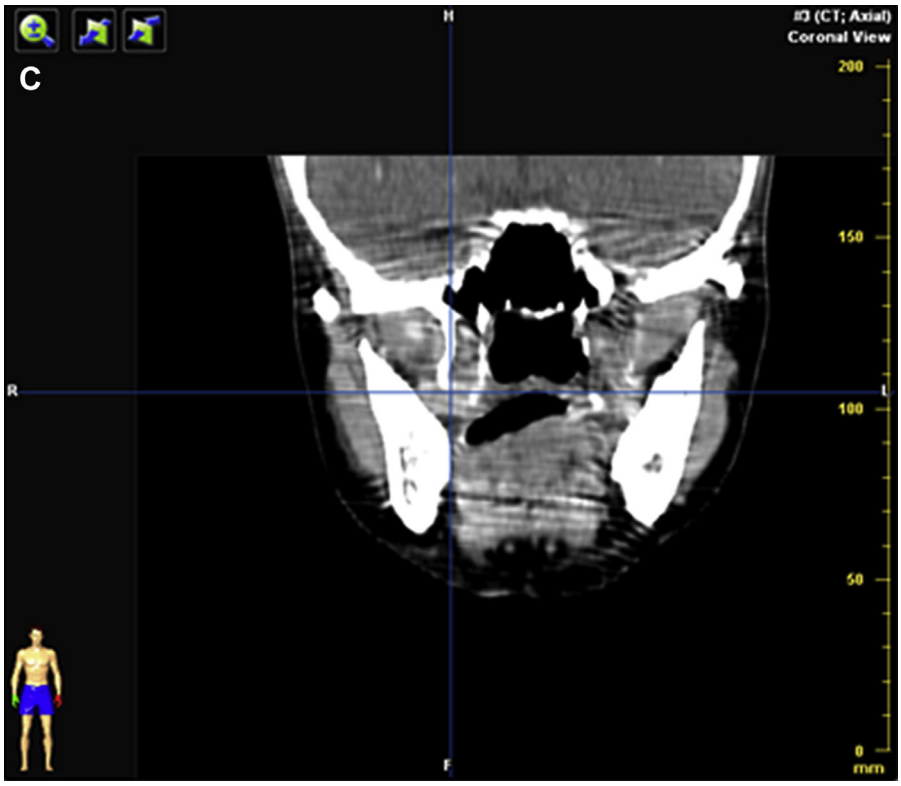

FIGURE 1 (cont'd). *C*, Coronal view of CECT.

Yu et al. Computer-Assisted Planning of Maxillectomy. J Oral Maxillofac Surg 2017.

in AutomA mode (range, 30 to 170 mA); the scan parameters were as follows: 140 keV; collimation, 3.75 mm; table feed, 17.50 mm/rotation; and slice thickness, 2.5 mm with 2.5-mm spacing. Three-dimensional PET images of the head and neck were then acquired for 2.5 minutes per frame, with an overlap of 9 slices between frames. CT-based attenuation-corrected PET images were reconstructed by use of a 3D iterative algorithm (VUE Point; GE Healthcare) and displayed as a 128 × 128 matrix (3.90 × 3.90 mm; slice thickness, 3.27 mm). Finally, maxillofacial CECT scans with a 1-mm slice thickness were acquired (field of view, 20 cm; pitch, 1.0; slice, 0.75 mm; 120 kV; 280 mA).

IMAGE FUSION

PET/CT and CECT datasets were transferred to the navigation system (iPlan 3.0; Brainlab, Feldkirchen, Germany) as standard DICOM (Digital Imaging and Communications in Medicine) files, and after matching of the landmarks, image fusion was performed on the workstation of the navigation system. The target could be visualized in multiplanar image reformations, allowing exact anatomic localization of the areas of enhanced tracer activity on the co-registered CECT images (Fig 3).

ACCURACY VERIFICATION

After image fusion, the PET/CT imaging and CECT imaging were in the same reference frame. Two 3D models of the skull were created from the PET/CT and CECT data by the navigation system and exported to Geomagic Studio 7 software (Raindrop Geomagic, Durham, NC). The average shift of the skull was calculated automatically (Fig 4).

TUMOR-MAPPING TECHNIQUE OF PET/CT

This image fusion technique allowed the abnormal uptake area to be exhibited on the CECT data. The hypermetabolic region was marked by the object creation function of the navigation system (Fig 5).

THREE-DIMENSIONAL CT IMAGING OF VESSELS

During the image fusion procedure, preoperative maxillofacial CECT data were imported into iPlan 3.0 software. Bilateral cervical vessels, the mandible, and the maxilla were marked using the navigation software. The 3D reconstruction images of vessels clearly showed the vascular diameters and locations, which helped select the most suitable vein and artery for anastomosis and defined the relationship between the recurrent tumor and critical structures. The right internal jugular vein had been sacrificed

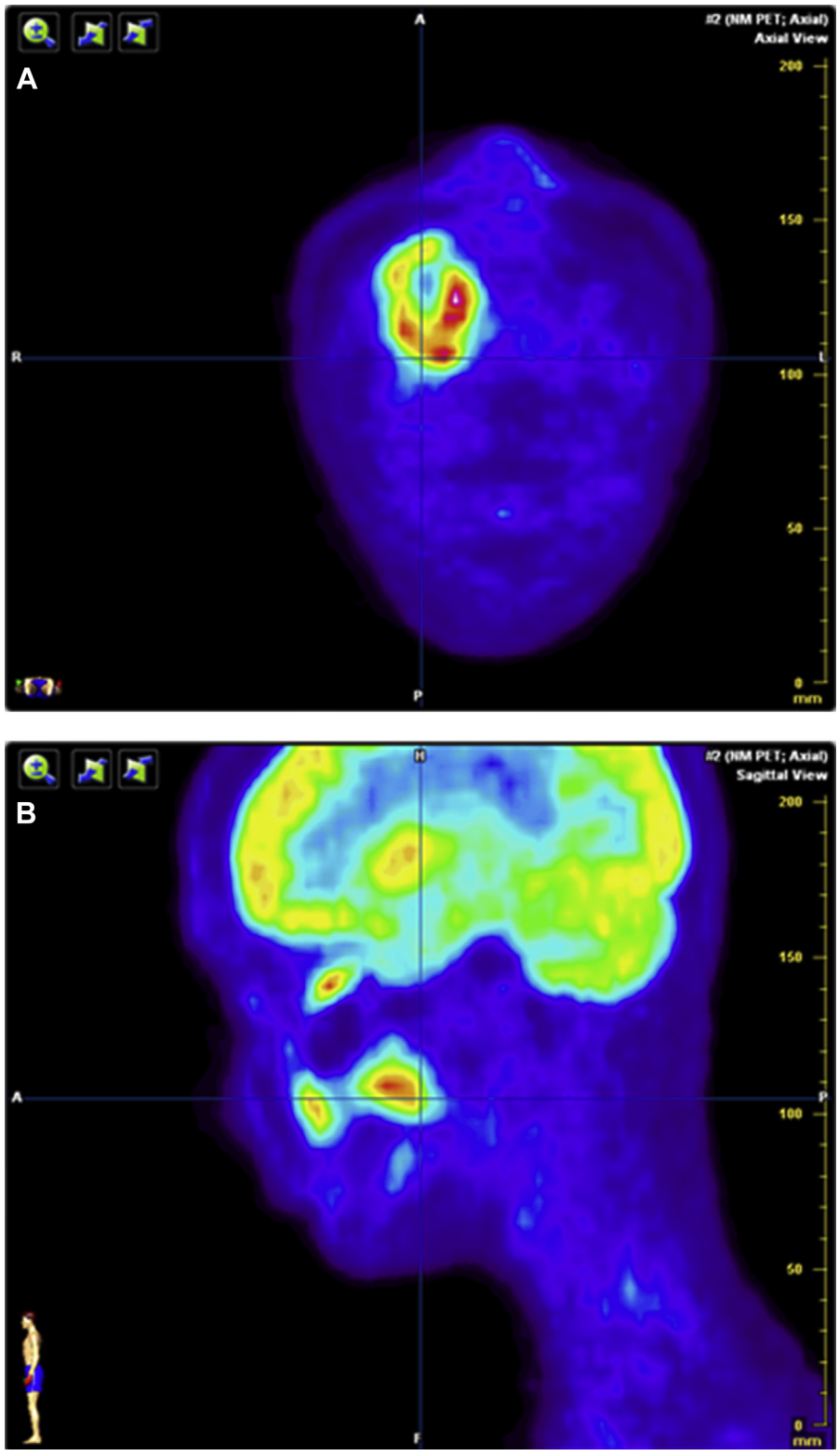

FIGURE 2. F-18 fluorodeoxyglucose (FDG) positron emission tomography (PET)/computed tomography (CT) scan showing well-defined tracer accumulation in the right skull-base region, close to the sphenoid sinus. *A*, Axial view of FDG-PET/CT. *B*, Sagittal view of FDG-PET/CT. **(Fig 2 continued on next page.)**

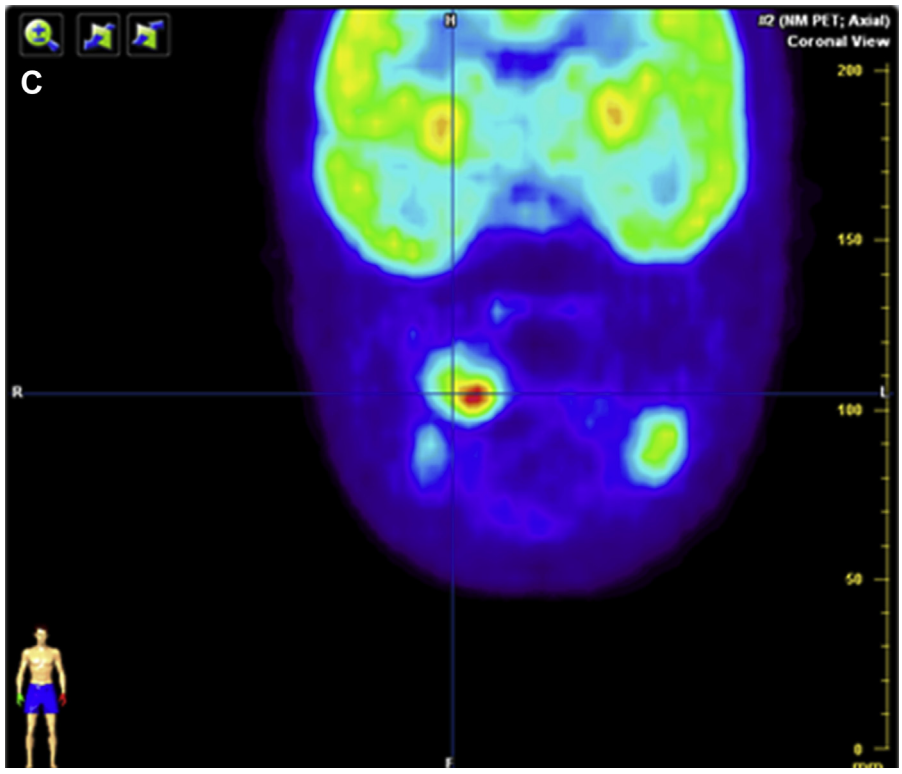

FIGURE 2 (cont'd). *C*, Coronal view of FDG-PET/CT.

Yu et al. Computer-Assisted Planning of Maxillectomy. J Oral Maxillofac Surg 2017.

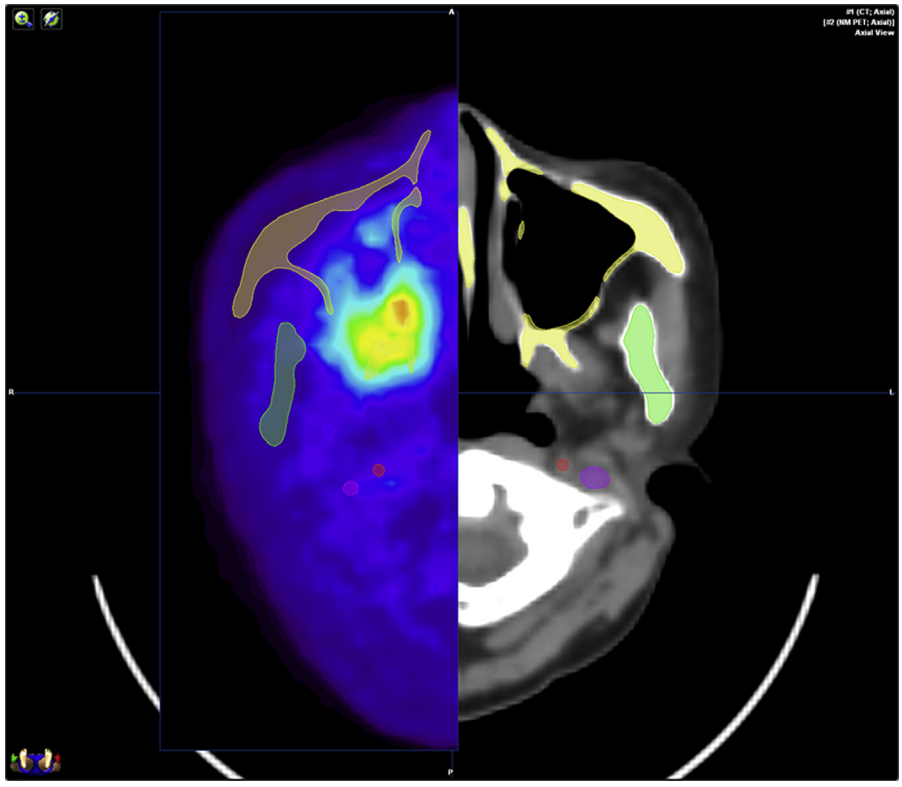

FIGURE 3. Image fusion of ^{18}F-fluorodeoxyglucose–positron emission tomography/computed tomography and contrast-enhanced computed tomography on the workstation of the navigation system (iPlan 3.0).

Yu et al. Computer-Assisted Planning of Maxillectomy. J Oral Maxillofac Surg 2017.

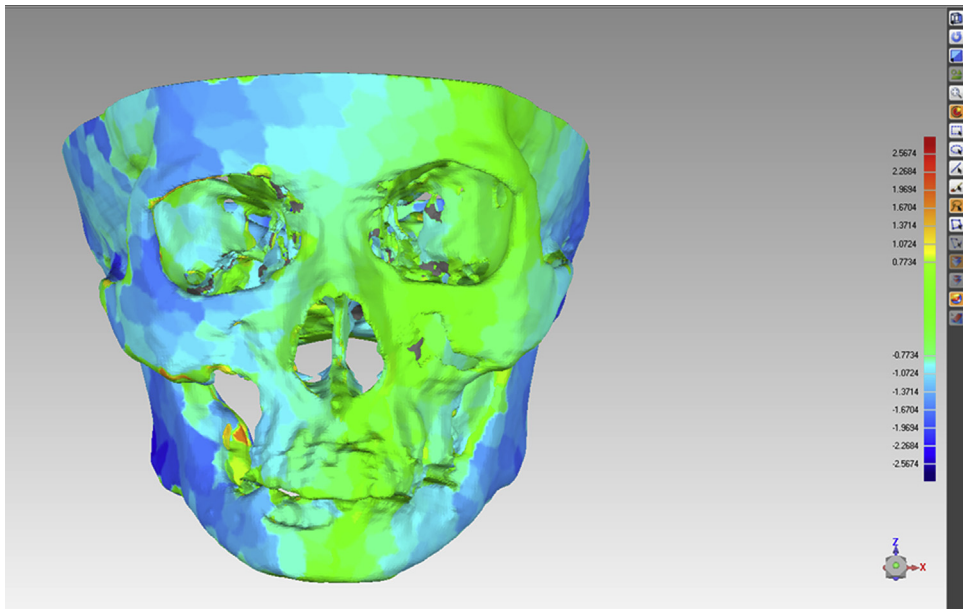

FIGURE 4. Accuracy verification of image fusion of ^{18}F-fluorodeoxyglucose–positron emission tomography/computed tomography by Geomagic Studio 7 software.

Yu et al. Computer-Assisted Planning of Maxillectomy. J Oral Maxillofac Surg 2017.

during the previous surgical procedure, but on the left side, the veins and arteries were in good condition; they were marked and prepared for anastomosis. Tumor mapping by PET/CT showed that the recurrent tumor was not close to the right internal carotid artery (Fig 6).

VIRTUAL PLANNING

SurgiCase CMF (Materialise, Leuven, Belgium) was used for surgical planning. CECT data of the maxillofacial skeleton were imported into SurgiCase CMF, and 3D virtual models of the maxilla and mandible were created. The virtual model of the tumor and maxilla created by the navigation system also was imported into SurgiCase CMF as standard stereolithograph files. The registration function was used to accurately determine tumor position. With the position of these 2 maxillae fixed, the position of the tumor in the CECT image was determined. Maxillary osteotomies were completed according to the extent of the tumor (Fig 7). The position of the osteotomy line and other details were provided to the surgeon. The information could be imported into the navigation system and used for navigation surgery. The flow diagram in Figure 8 shows the process of 3D image fusion of FDG-PET/CT and CECT.

Ethical approval was given for our study (document No. PKUSSIRB-201522051). This study features a human patient, and we confirm that we have read the Helsinki Declaration and have followed the guidelines in this investigation.

Results

In our patient, the left facial vein and artery were used for anastomosis with the donor vessels through the soft palate and parapharyngeal space (Fig 9). Pathologic examination showed negative tumor margins, and the free anterolateral thigh flap survived successfully, without any complications. The shift of the 3D image fusion between FDG-PET/CT and CECT was 0.77 ± 0.53 mm. Our technique could precisely visualize the metabolic tumor volume and reconstruct the recipient vessels to accomplish resection and reconstruction of recurrent maxillary SCC.

Discussion

Treatment of recurrent maxillary SCC is challenging because tissue distortion as a result of previous surgery and radiotherapy makes accurate identification of the tumor and the relationship to nearby critical structures difficult. To overcome this problem, we attempted a new technique of 3D image fusion of FDG-PET/CT and CECT for computer-assisted planning of resection of recurrent maxillary SCC and defect reconstruction in a 46-year-old woman.

FDG-PET has recently been shown to be very useful for staging of head and neck cancer,[3] as it can identify the primary lesion, nodal involvement, distant metastasis, and secondary tumors. It has high sensitivity and specificity in detection of nodal metastases[4,6,9] and can differentiate residual or recurrent disease from normal treatment-induced tissue changes.[7]

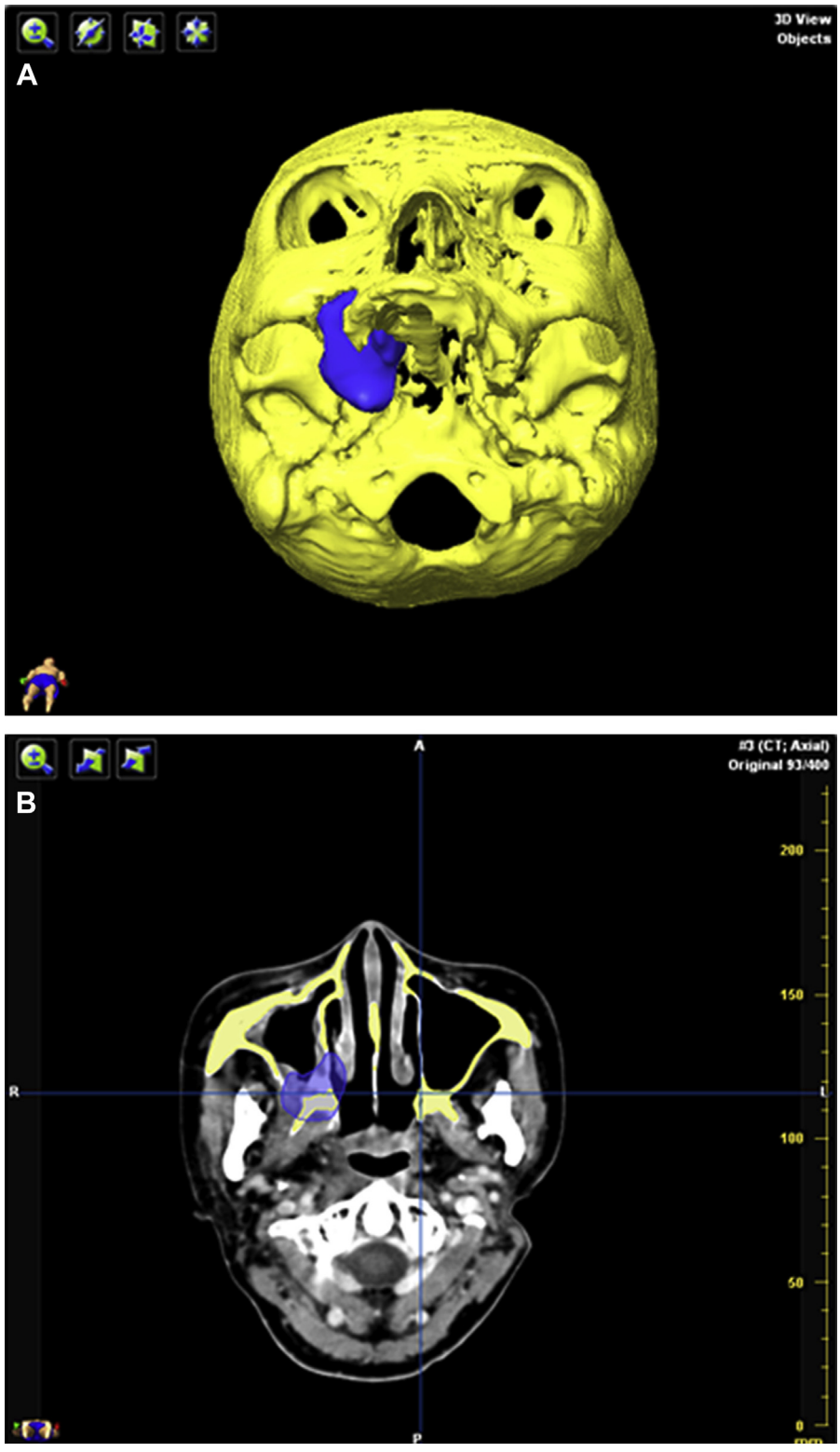

FIGURE 5. Tumor mapping according to the hypermetabolic region by the object creation function of the navigation system (iPlan 3.0). *A*, Three-dimensional simulation showing the relationship between the tumor and maxilla. *B*, Axial view of tumor mapping. **(Fig 5 continued on next page.)**

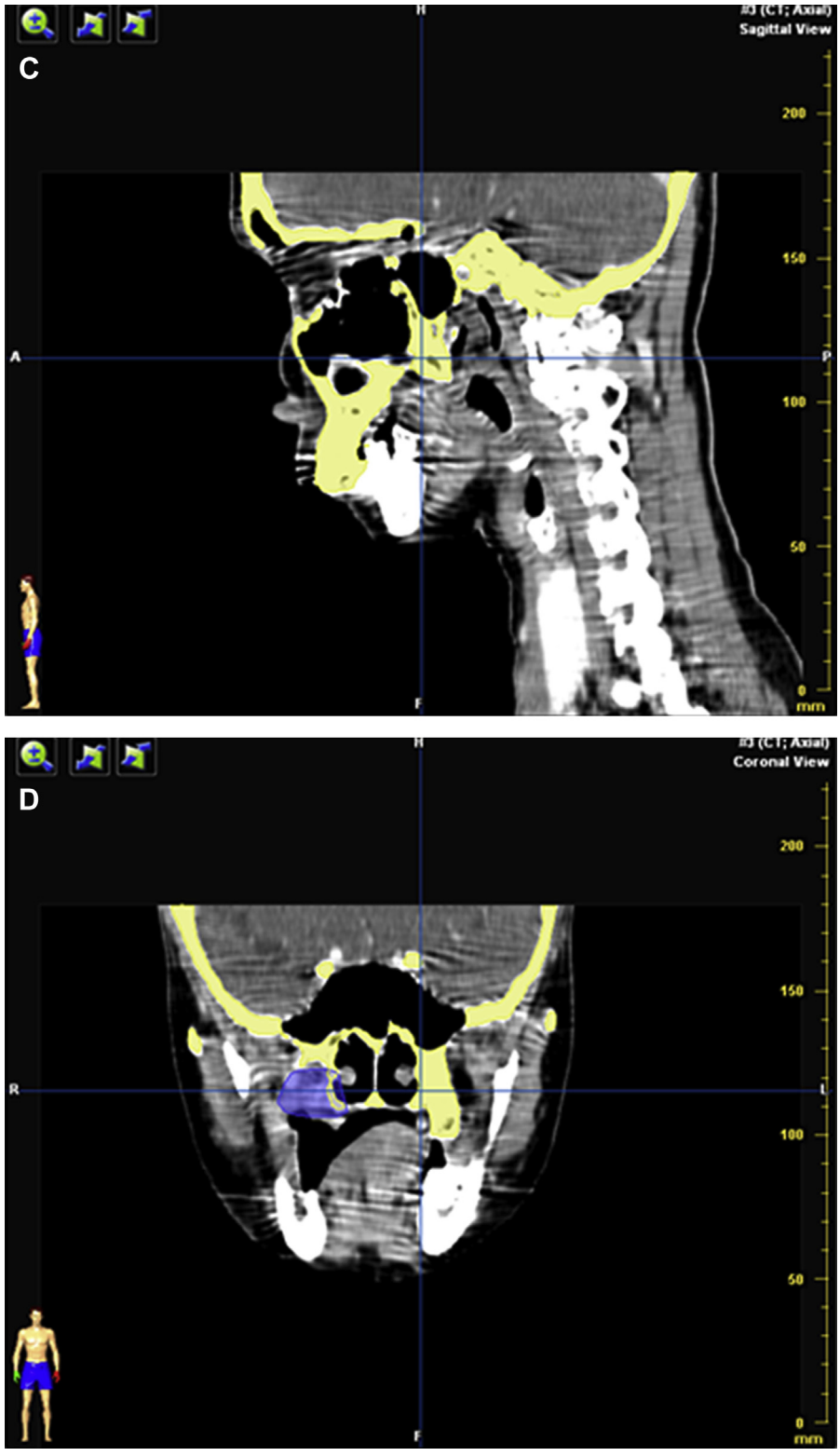

FIGURE 5 (cont'd). *C*, Sagittal view of tumor mapping. *D*, Coronal view of tumor mapping.

Yu et al. Computer-Assisted Planning of Maxillectomy. J Oral Maxillofac Surg 2017.

Combined PET-CT scanning has been introduced recently; it provides anatomic information from the CT scan in conjunction with the functional information from the PET scan. Historically, PET has not been as effective for T classification as it has been for nodal staging, primarily because it does not provide anatomic

FIGURE 6. Computed tomography 3-dimensional imaging of vessels from contrast-enhanced computed tomography data. *A*, Three-dimensional simulation showing the relationship among the vessels, tumor, and maxilla. *B*, Axial view of vessel imaging. **(Fig 6 continued on next page.)**

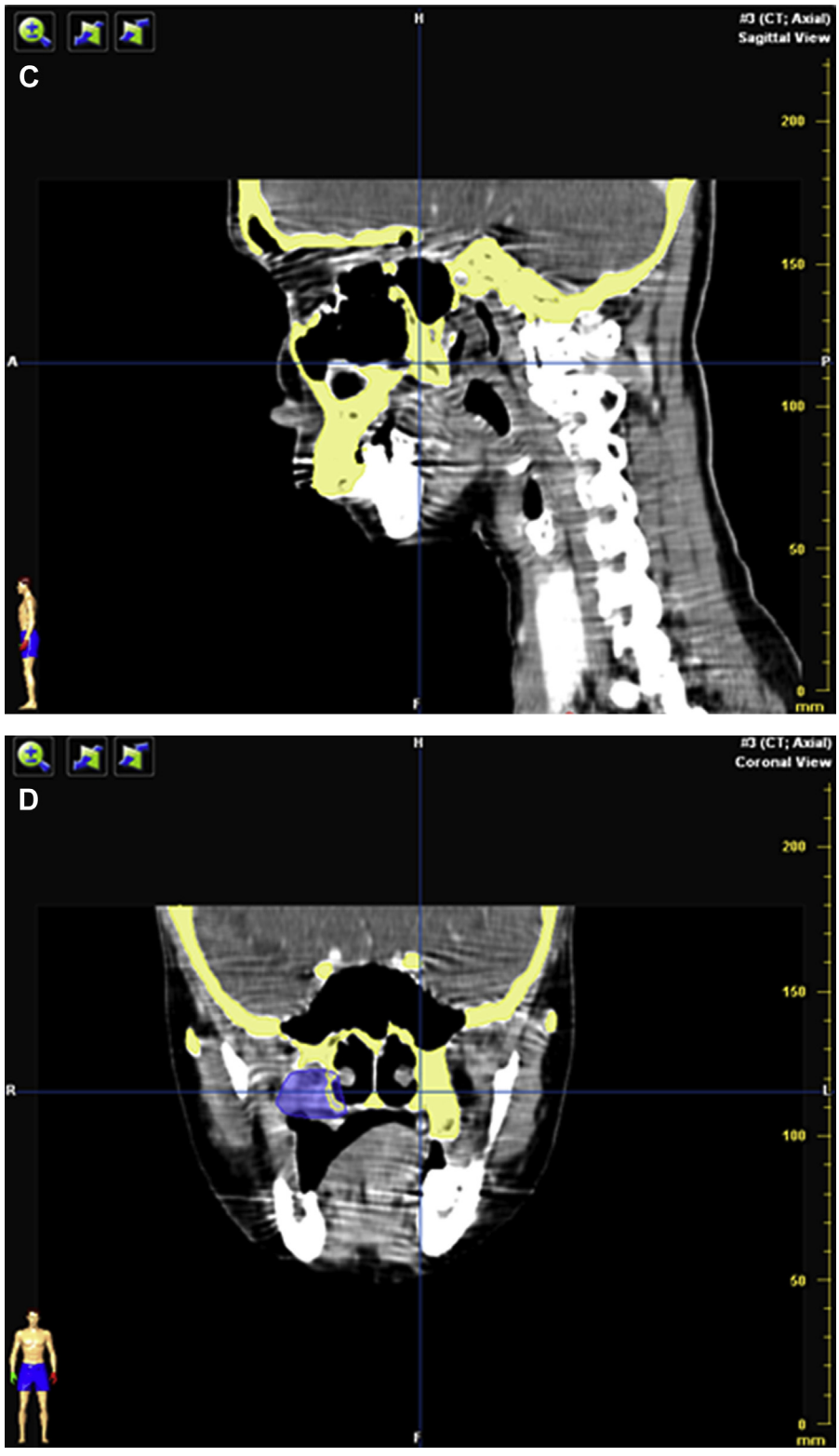

FIGURE 6 (cont'd). *C*, Sagittal view of vessel imaging. *D*, Coronal view of vessel imaging.

Yu et al. Computer-Assisted Planning of Maxillectomy. J Oral Maxillofac Surg 2017.

information. PET-CT, on the other hand, provides critical structural anatomic information about the tumor and its relationship to adjacent soft tissue and surrounding bone, muscle, and cartilage. It allows functional imaging to become a component of radiation treatment planning. The fused image provides

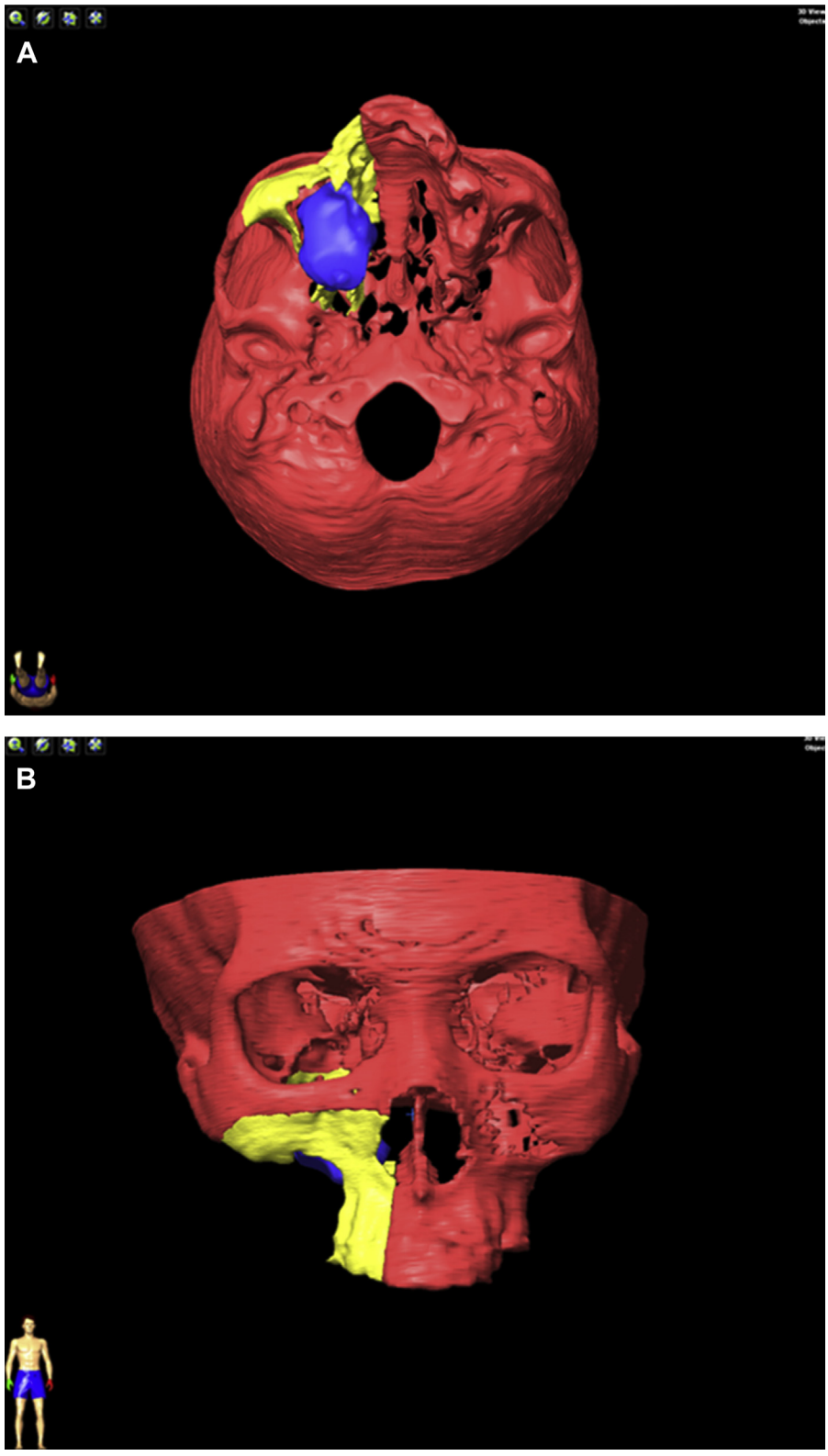

FIGURE 7. Simulation of virtual osteotomy on SurgiCase workstation. *A*, Three-dimensional simulation showing the osteotomy line of the hard palate. *B*, Three-dimensional simulation showing the suborbital osteotomy line. **(Fig 7 continued on next page.)**

Yu et al. Computer-Assisted Planning of Maxillectomy. J Oral Maxillofac Surg 2017.

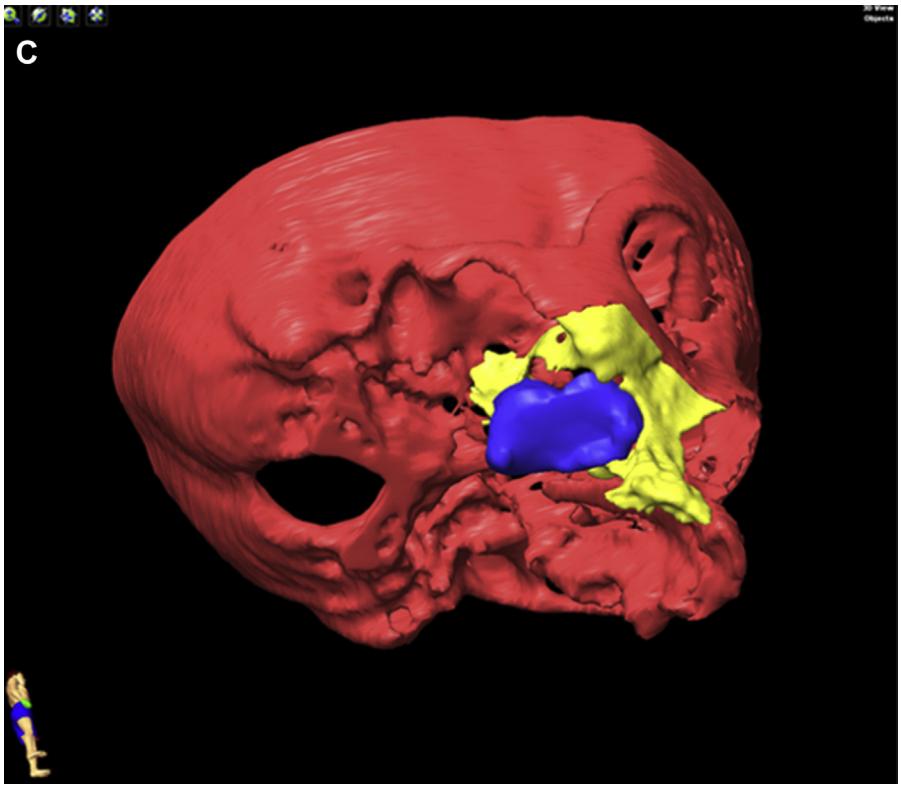

FIGURE 7 (cont'd). *C*, Three-dimensional simulation showing the zygomatic osteotomy line.

Yu et al. Computer-Assisted Planning of Maxillectomy. J Oral Maxillofac Surg 2017.

the anatomic delineation of the tumor, as well as biological information, which is useful for identifying target volumes.[10,11]

FDG-PET combined with CT is now an important tool for oncologic staging and response assessment.[10] In one study, the combination of FDG-PET/CT with native CT enabled accurate diagnosis of 93% of lesions in 90% of patients with head and neck cancers.[11] An increased glucose metabolic rate is characteristic of most malignant cells and shows the biochemical differences between malignant and normal tissue.[12] A major disadvantage of FDG-PET, however, is that it yields only

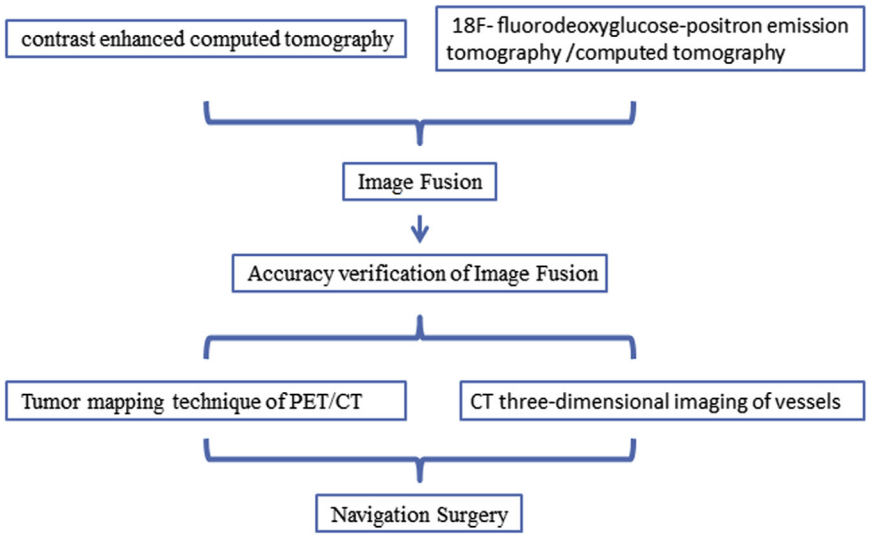

FIGURE 8. Flow diagram for 3-dimensional image fusion of ^{18}F-fluorodeoxyglucose–positron emission tomography (PET)/CT and contrast-enhanced CT for computer-assisted planning of maxillectomy of recurrent maxillary squamous cell carcinoma and defect reconstruction.

Yu et al. Computer-Assisted Planning of Maxillectomy. J Oral Maxillofac Surg 2017.

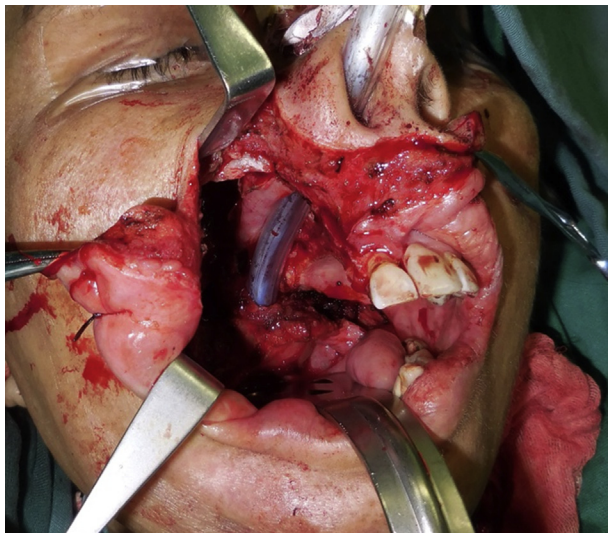

FIGURE 9. Intraoperative photograph of patient showing the soft palate and parapharyngeal space used to connect donor vessels to the left facial vein and artery.

Yu et al. Computer-Assisted Planning of Maxillectomy. J Oral Maxillofac Surg 2017.

limited information on the anatomic location of the lesion. To resolve this problem, we decided to use PET/CT image fusion not only as a diagnostic tool, but also as a reference imaging modality for image-guided tumor mapping.

Although PET/CT, with the near synchronous image acquisition and exact co-registration of anatomic and metabolic data, enables accurate anatomic localization of PET abnormalities and more confident PET interpretations, it provides little information regarding the vessels around the tumor region. Especially for recurrent tumor, the metabolic tumor and the critical vessels around the tumor cannot appear at the same time in the same imaging examination. For this reason, combined PET/CT and CECT can address this problem.

For the patient in this study, the extent of the recurrent tumor was difficult to identify with magnetic resonance imaging/CECT, but the vessels around the tumor could be well demonstrated. With 3D image fusion of FDG-PET/CT and CECT, the extent of the recurrent tumor and the vessels around the tumor can be visualized in the same reference frame, and this can be used for the virtual plan and navigation surgery.

Definitive surgical resection of locally advanced SCC of the head and neck frequently results in complex bone and soft tissue defects, but these can be reliably repaired with free tissue transfer reconstruction with microvascular anastomosis. Comprehensive treatment of advanced head and neck cancers frequently mandates the use of definitive or adjuvant external beam radiation therapy (XRT). However, radiation therapy can damage small vessels and adversely affect microvascular anastomoses. Specifically, XRT causes diminished smooth muscle density, endothelial cell dehiscence, and vessel wall fibrosis.[13,14] Krag et al[15] showed that administering XRT to recipient vessels in rabbits before surgery markedly increased free flap failure rates. Studies by other groups have not supported these findings,[16,17] and controversy still persists as to the exact effect of XRT on the rate and severity of local surgical bed complications after free tissue transfers.[18]

Survival of the flap relies on successful vessel anastomosis, which makes it paramount to optimize anatomic orientation and minimize torsion or kinking.[19] Many studies have reported a significant association between previous surgery and anastomosis insufficiencies.[20-22] In recurrent maxillary SCC, reconstruction can be challenging because of the soft tissue scarring and absence of suitable recipient vessels as a result of previous surgery and radiotherapy. Combined free flaps and flow-through or chain-link flaps have been recommended as alternative approaches for bone and oral linings in secondary reconstruction, particularly for patients in whom suitable recipient vessels in the facial region cannot be identified.[23,24] Keles et al[25] defined the different courses and percentages of the hepatic artery detected during preoperative evaluation of living liver donors using multidetector CT angiography.

The patient in our study had undergone tumor resection followed by radiation therapy 15 years earlier, and the right internal jugular vein and facial and lingual arteries were blocked. This left us with 3 options: *1)* choose the ipsilateral superficial temporal vessels as the recipient vessels, *2)* go through the ipsilateral submandibular and submental space, or *3)* choose the left facial artery and vessel for anastomosis through the soft palate and parapharyngeal space.

Three-dimensional CT images of blood vessels were acquired to determine the most suitable recipient vessels with regard to position and diameter. The right superficial temporal artery was reconstructed by the software, but the diameter and position were not fit for anastomosis with the lateral femoral circumflex artery. Las et al[26] found that free flaps anastomosed to the superficial temporal artery had a 4.4 times greater risk of total flap necrosis. Although this artery is easily accessible because of its superficial location, its diameter may be insufficient and vasospasm may easily develop. For scalp reconstruction, however, we prefer superficial temporal vessels as the recipient vessels because of their proximity. To prevent insufficient flow, these vessels must be dissected farther proximal into the parotid gland in front of the tragus, where their caliber in general is large.[26] Most complications of free fibular flap reconstruction involve vascular compromise, and evaluation of the vascular anatomy

can potentially minimize these complications. CT angiography data have been reported to be particularly useful.[27,28] In our patient, 3D CT images of blood vessels were acquired to determine the most suitable recipient vessels with regard to position and diameter. Visualization of the vessels can help the surgeon select suitable vessels for anastomosis and estimate the approximate length of the vessel pedicle, thus avoiding the need for placing multiple incisions for exposure. In our patient, the diameter and position of the right superficial temporal artery were not fit for anastomosis with the lateral femoral circumflex artery, and the vessel pedicle of the left submandibular vessels was too short to permit connection between the right maxilla and the left submandible by the conventional methods. We therefore chose the left facial artery and vessel for anastomosis through the soft palate and parapharyngeal space. This channel is considered the first choice for accommodation of the vessel pedicles as it considerably shortens the distance between the right maxilla and the left submandible.

In this article we have described a new method for resection and reconstruction of recurrent maxillary SCC using 3D image fusion of FDG-PET/CT and CECT. The method can be used for anatomic localization of the recurrent cancer, critical nearby structures, and the recipient vessel for reconstruction. This method has the potential to improve clinical outcomes in patients with recurrent maxillary SCC.

Acknowledgment

We appreciate the professional editor at Elixigen for revising and modifying the English language of this manuscript.

References

1. Bailet JW, Mark RJ, Abemayor E, et al: Nasopharyngeal carcinoma: Treatment results with primary radiation therapy. Laryngoscope 102:965, 1992
2. Perez CA, Devineni VR, Marcial-Vega V, et al: Carcinoma of the nasopharynx: Factors affecting prognosis. Int J Radiat Oncol Biol Phys 23:271, 1992
3. Koshy M, Paulino AC, Howell R, et al: F-18 FDG PET-CT fusion in radiotherapy treatment planning for head and neck cancer. Head Neck 27:494, 2005
4. Kau RJ, Alexiou C, Laubenbacher C, et al: Lymph node detection of head and neck squamous cell carcinomas by positron emission tomography with fluorodeoxyglucose F 18 in a routine clinical setting. Arch Otolaryngol Head Neck Surg 125:1322, 1999
5. Wong WL, Chevretton EB, McGurk M, et al: A prospective study of PET-FDG imaging for the assessment of head and neck squamous cell carcinoma. Clin Otolaryngol Allied Sci 22:209, 1997
6. Laubenbacher C, Saumweber D, Wagner-Manslau C, et al: Comparison of fluorine-18-fluorodeoxyglucose PET, MRI and endoscopy for staging head and neck squamous-cell carcinomas. J Nucl Med 36:1747, 1995
7. Schechter NR, Gillenwater AM, Byers RM, et al: Can positron emission tomography improve the quality of care for head-and-neck cancer patients? Int J Radiat Oncol Biol Phys 51:4, 2001
8. Sironi S, Buda A, Picchio M, et al: Lymph node metastasis in patients with clinical early-stage cervical cancer: Detection with integrated FDG PET/CT. Radiology 238:272, 2006
9. McGuirt WF, Williams DW, Keyes JW, et al: A comparative diagnostic study of head and neck nodal metastases using positron emission tomography. Laryngoscope 105:373, 1995
10. Czernin J, Benz MR, Allen-Auerbach MS: PET/CT imaging: The incremental value of assessing the glucose metabolic phenotype and the structure of cancers in a single examination. Eur J Radiol 73:470, 2010
11. Feichtinger M, Pau M, Zemann W, et al: Intraoperative control of resection margins in advanced head and neck cancer using a 3D-navigation system based on PET/CT image fusion. J Craniomaxillofac Surg 38:589, 2010
12. Feichtinger M, Aigner RM, Karcher H: F-18 positron emission tomography and computed tomography image-fusion for image-guided detection of local recurrence in patients with head and neck cancer using a 3-dimensional navigation system: A preliminary report. J Oral Maxillofac Surg 66:193, 2008
13. De Wilde RL, Donders G: Scanning electron microscopic study of microvascular anastomoses on irradiated vessels: Long-term effect of irradiation. Microsurgery 7:156, 1986
14. Guelinckx PJ, Boeckx WD, Fossion E, et al: Scanning electron microscopy of irradiated recipient blood vessels in head and neck free flaps. Plast Reconstr Surg 74:217, 1984
15. Krag C, De Rose G, Lyczakowski T, et al: Free flaps and irradiated recipient vessels: An experimental study in rabbits. Br J Plast Surg 35:328, 1982
16. Cunningham BL, Shons AR: Free flap transfers in rats using an irradiated recipient site. Br J Plast Surg 32:137, 1979
17. Bengtson BP, Schusterman MA, Baldwin BJ, et al: Influence of prior radiotherapy on the development of postoperative complications and success of free tissue transfers in head and neck cancer reconstruction. Am J Surg 166:326, 1993
18. Choi S, Schwartz DL, Farwell DG, et al: Radiation therapy does not impact local complication rates after free flap reconstruction for head and neck cancer. Arch Otolaryngol Head Neck Surg 130:1308, 2004
19. Modest MC, Moore EJ, Abel KM, et al: Scapular flap for maxillectomy defect reconstruction and preliminary results using three-dimensional modeling. Laryngoscope 127:E8, 2016
20. Cloke DJ, Green JE, Khan AL, et al: Factors influencing the development of wound infection following free-flap reconstruction for intra-oral cancer. Br J Plast Surg 57:556, 2004
21. Disa JJ, Pusic AL, Hidalgo DH, et al: Simplifying microvascular head and neck reconstruction: A rational approach to donor site selection. Ann Plast Surg 47:385, 2001
22. Singh B, Cordeiro PG, Santamaria E, et al: Factors associated with complications in microvascular reconstruction of head and neck defects. Plast Reconstr Surg 103:403, 1999
23. Antony AK, Chen WF, Kolokythas A, et al: Use of virtual surgery and stereolithography-guided osteotomy for mandibular reconstruction with the free fibula. Plast Reconstr Surg 128:1080, 2011
24. Ceulemans P, Hofer SO: Flow-through anterolateral thigh flap for a free osteocutaneous fibula flap in secondary composite mandible reconstruction. Br J Plast Surg 57:358, 2004
25. Keles P, Yuce I, Keles S, et al: Evaluation of hepatic arterial anatomy by multidetector computed tomographic angiography in living donor liver transplantation. Biochem Genet 54:283, 2016
26. Las DE, de Jong T, Zuidam JW, et al: Identification of independent risk factors for flap failure: A retrospective analysis of 1530 free flaps for breast, head and neck and extremity reconstruction. J Plast Reconstr Aesthet Surg 69:894, 2016
27. Sakakibara S, Onishi H, Hashikawa K, et al: Three-dimensional venous visualization with phase-lag computed tomography angiography for reconstructive microsurgery. J Reconstr Microsurg 31:305, 2015
28. Garvey PB, Chang EI, Selber JC, et al: A prospective study of preoperative computed tomographic angiographic mapping of free fibula osteocutaneous flaps for head and neck reconstruction. Plast Reconstr Surg 130:541e, 2012